

9-27-2020

## Experimental study on wetting front migration induced by rainfall infiltration in unsaturated slope wash and residual soil

Wen-bin JIAN

*Engineering Research Center of Geological Engineering, Fuzhou University, Fujian 350108, China*

Cong-hui HUANG

*Department of Geotechnical and Geological Engineering, Fuzhou University, Fuzhou, Fujian 350108, China*

Yang-hua LUO

*Department of Geotechnical and Geological Engineering, Fuzhou University, Fuzhou, Fujian 350108, China*

Wen NIE

*Quanzhou Institute of Equipment Manufacturing, Haixi Institute, Chinese Academy of Sciences, Quanzhou, Fujian 362200, China*

Follow this and additional works at: <https://rocksoilmach.researchcommons.org/journal>



Part of the [Geotechnical Engineering Commons](#)

---

### Custom Citation

JIAN Wen-bin, HUANG Cong-hui, LUO Yang-hua, NIE Wen, . Experimental study on wetting front migration induced by rainfall infiltration in unsaturated slope wash and residual soil[J]. Rock and Soil Mechanics, 2020, 41(4): 1123-1133.

This Article is brought to you for free and open access by Rock and Soil Mechanics. It has been accepted for inclusion in Rock and Soil Mechanics by an authorized editor of Rock and Soil Mechanics.

## Experimental study on wetting front migration induced by rainfall infiltration in unsaturated slope wash and residual soil

JIAN Wen-bin<sup>1,2</sup>, HUANG Cong-hui<sup>1</sup>, LUO Yang-hua<sup>1</sup>, NIE Wen<sup>3</sup>

1. Department of Geotechnical and Geological Engineering, Fuzhou University, Fuzhou, Fujian 350108, China

2. Engineering Research Center of Geological Engineering, Fuzhou University, Fujian 350108, China

3. Quanzhou Institute of Equipment Manufacturing, Haixi Institute, Chinese Academy of Sciences, Quanzhou, Fujian 362200, China

**Abstract:** Rain infiltration through the soil is the critical factor in the frequent landslides on the coast of China. By considering the geological disaster points of Dehua County, Quanzhou City, Fujian Province as the main research object, the permeability characteristics of slope wash and granite residual soil are concerned in these typical geological disaster points. The one-dimensional soil column infiltration test was carried out using the soil infiltration device developed by simulating rain intensities of 15, 30 and 60 mm/h, respectively, with the rainfall conditions of duration (180 min) and amount (90 mm). The response law of moisture content, wetting front and infiltration rate of each soil column with time under different working conditions was investigated. The main results are presented in detail. The soil wetness spreads deeper and faster as the permeability coefficient of soil and the rainfall intensity become greater. The soil moisture content responds to rainfall from shallow to deep part during the process of rainfall infiltration. Meanwhile, the influence of different rain intensities on water content is mainly reflected in the first response time and saturation time. The high intensity of rain leads to short response time and a quick saturation speed. A function is proposed for different rainfall intensities, which can characterise the wetting front infiltration laws of the Maping landslide and the Bengtuling landslide in Dehua County. The results are of great significance for the early warning of landslide hazards.

**Keywords:** rainfall; slope wash and residual soil; wetting front; response time; landslide

### 1 Introduction

In the southeast coastal area of China, the mountain hills are well developed with abundant rainfall. The slope surfaces are often covered by the eluvial and residual soil layers, and the structure of the slopes is loose. There are many geological disasters, including landslides and debris flows under the invasion of meteorological disasters such as typhoon and rainstorm. The rainwater infiltrating into the soil during rainfall is the key factor leading to the deformation, damage of the soil slope and the occurrence of debris flow. Therefore, the research on the characteristics of soil rainfall infiltration and the law of wetting front migration for the eluvial and residual soil, from unsaturated state to saturated state under rainfall infiltration, will be significant to further reveal the development mechanism of soil landslide and debris flow.

So far, scholars have conducted a lot of research on the mechanism of landslides induced by rainfall infiltration. Relying on the meteorological data in Hong Kong, Lumb<sup>[1]</sup> studied the relationship between landslides and rainfall, and proposed an infinite slope method to analyze slope stability. Through establishing a simplified one-dimensional vertical rainfall infiltration model, the advancing speed of wetting front and the redistribution of moisture content were determined. According to the empirical relationship between the shear

strength and the saturation of the soil, the slope stability under different geological conditions and rainfall characteristics was analyzed on the assumption that the failure surface was parallel to the slope. Li et al.<sup>[2]</sup> adopted the measured data to analyze the slope stability using the infinite slope method, avoiding the error caused by the infiltration model when deducing the water content distribution. On the basis of Lumb's method, Yan et al.<sup>[3]</sup> developed a calculation method of slope stability under rainfall combined with the one-dimensional consolidation theory of Terzaghi. Yeh et al.<sup>[4]</sup> used Philips' infiltration model as the rainfall infiltration model to analyze the slope stability by the infinite slope method. Li et al.<sup>[5]</sup> improved the Mein-Larson rainfall infiltration model with the unsaturated soil VG model and the improved Green-Ampt infiltration model, which optimized the infinite slope model. Compared with the existing simplified models, this model took into account not only the impact of the slope inclination, but also the characteristics of unsaturated soil, which was more adaptable to the different rainfall patterns, and provided a feasible method for rapid approximate estimation of rainfall-induced landslides, with a wider application range. Han et al.<sup>[6]</sup> adopted the Green-Ampt infiltration model considering the closed air pressure factor as the rainfall infiltration model, and analyzed the change of the safety factor of slope with time. He found that the air pressure had a significant delayed effect on the reduction of factor of

Received: 11 March 2019

Revised: 20 June 2019

This work was supported by the National Natural Science Foundation of China (41861134011).

First author: JIAN Wen-bin, male, born in 1963, PhD, Professor, research interests: Geotechnical engineering and engineering geology. E-mail: [jwb@fzu.edu.cn](mailto:jwb@fzu.edu.cn)

safety under the condition of heavy rainfall.

In terms of research on the development mechanism of landslide by the field rainfall tests, Wen et al.<sup>[7]</sup> used a new type of landslide monitoring system to explore the relationship between rainfall, infiltration, and displacement deformation, and also revealed the variation characteristics of the infiltration depth of the landslide under certain rainfall. Zhou et al.<sup>[8]</sup> carried out monitoring tests on Qinglong landslide in Guizhou province to study the deformation and displacement characteristics of the landslide during rainfall. Li et al.<sup>[9]</sup> conducted artificial rainfall simulation tests on a highway slope, and monitored the pore water pressure, slope earth pressure, and deformation of the slope soil, and also discussed the influence of rainwater infiltration on the stability of the embankment slope. Zheng et al.<sup>[10]</sup> undertook the on-site observations of the high slope under rainfall infiltration, and studied the variations of the slope displacement, groundwater level and soil matrix suction with rainfall. They found that long-term continuous rainfall has a great impact on the slope stability. Zhan et al.<sup>[11]</sup> selected typical landslides in Zaoyang, Hubei province to conduct artificial rainfall simulation tests on site, and discussed the variation characteristics of the pore water pressure during the process of rainfall infiltration.

In conclusion, the current researches mentioned above mainly focus on the relationship between rainfall (or rainfall intensity) and landslide deformation, pore water pressure, earth pressure, etc. However, the research on the change of soil infiltration performance and water redistribution caused by rainfall is still not in-depth. Moreover, the column tests mostly use the disturbed soil<sup>[12–15]</sup>, and it is rare to collect the undisturbed soil pillars on site to conduct tests. Therefore, in this paper, the self-developed rainfall test and soil column infiltration test devices were used to carry out one-dimensional soil column infiltration test on the undisturbed granite eluvial and residual soil, and analyzed the infiltration performance of unsaturated eluvial and residual soil under the condition of rainfall in the research area. This study can provide the theoretical basis for further revealing the disaster-pregnancy mechanism of rainfall-induced landslides and monitoring and early warning.

## 2 Rainfall infiltration test of undisturbed soil column

### 2.1 Test soil

The soil samples were collected from two geological disaster points, namely the Maping landslide in Shangyong town and the Neiban landslide in Guobao town, Dehua county, Fujian province. For each geological point, two sets of undisturbed large-diameter soil columns were collected (a total of 4 samples), as are shown in Fig. 1.

During the sampling process, plenty of soil near the soil column was firstly dug out using hoes and shovels, and the

large pieces of the soil were cut off by knives. After gradually approaching the range of the soil column, the side-wall surface of the soil column was smoothed by a knife. In order to ensure that the soil sample could be smoothly pressed into the soil column barrel, the inner wall of the soil column bucket was smeared with vaseline. After the sample was collected, the cylinder mouths were wrapped with plastic film and sealed with packaging tape. The outer layer was wrapped with plastic film to reduce the evaporation of soil moisture in the barrel.



Fig.1 Sample photo of soil column

The physical and mechanical parameters of soil column are shown in Table 1.

Table 1 Physical and mechanical properties of rock-soil

Sampling points	Soil sample and number	Unit weight $\gamma/(\text{kN} \cdot \text{m}^{-3})$	Cohesion $c/\text{kPa}$	Internal friction angle $\varphi/(\text{°})$	Coefficient of permeability $K/(\text{cm} \cdot \text{s}^{-1})$	Moisture content $W/\%$	Void ratio $e$
Maping landslide	Slope wash soil (MP1)	17.5	27.4	15.3	$1.1 \times 10^{-6}$	25.7	0.87
	Residual soil (MP2)	19.2	22.3	19.9	$5.9 \times 10^{-4}$	23.3	0.83
Neiban landslide	Slope wash soil (NB1)	18.3	25.4	17.3	$5.2 \times 10^{-6}$	26.9	0.88
	Residual soil (NB2)	19.6	24.3	21.3	$3.5 \times 10^{-4}$	22.8	0.81

### 2.2 Test device

#### 2.2.1 Rainfall infiltration device

The infiltration device used in the experiment is shown in Fig. 2. The device is composed of four cylindrical soil column barrels made of plexiglass. The cross-section diameter, wall thickness and height of the soil column barrel are 35 cm, 0.5 cm, and 100 cm, respectively. In order to facilitate the observation of rainfall infiltration process in the soil and acquire the moisture content of soil samples at different depths, holes were made in one side of the soil column barrel to place the moisture sensors and further sealed. Considering that the slope gradient of the landslide surface from which the undisturbed soil was sampled is about 30°–35°, and the surface runoff could flow out of the slope easily and quickly, the overflow holes were set on the top of the barrel.



Fig.2 Soil column infiltration testing device

2.2.2 Rainfall simulation system

The rainfall simulation system mainly incorporates the rainfall device, water supply tank, water pump, main controller (data acquisition) and rain gauge, etc., as is illustrated in Fig.3. Among them, the rainfall device is composed of water supply pipeline, rain shower and pressure gauge. The rainfall intensity is regulated through different nozzles. During rainfall, the water was pumped from water storage tank (1 m in diameter and 2 m in height) to the rainfall device by water pump. The effective rainfall coverage area in the tests was 4–8 m<sup>2</sup> (changed with the rainfall intensity), and the variation range of rainfall intensity was 0–200 mm/h, where the variation range of stable rainfall intensity (high uniformity) was 15–120 mm/h, and the corresponding regulation accuracy was about 5 mm/h, which could meet the test requirements of the rainfall plans.



Fig.3 Main equipment of rainfall simulation

2.2.3 Data acquisition system and monitoring elements

For the data collection during the test, Hunan Xiangyinhe Automated Data Acquisition System was adopted to observe the data changes of each monitoring element in real time.

During the test, for each soil column, three moisture sensors, named D1, D2, and D3 were placed at 10 cm, 20 cm, and 30 cm away from the top of the barrel, respectively (shown in Figure 2). The MP-406B soil moisture sensor produced by Nantong Zhongtian was adopted. Its resolution was  $\pm 0.1\%$ , and the measurement accuracy was  $\pm 2\%$  (volume %), and the MP-406B moisture probe mainly measured the volume content of the water in the measured medium. The saturation standard of *Standard For Soil Test Method* (GB/T50123–1999) [16] was

used as the evaluation value of soil saturation in this test.

2.3 Rainfall plan

The climate of Dehua country belongs to subtropical mountain climate characterized with abundant rainfall and rain in hot season. The rainfall of the whole county ranges from 1301.5 mm to 2343.0 mm, and the average rainfall for many years is 1966.3 mm. Considering the typical climate characteristics and rainfall characteristics of the rainy seasons in this region, 3 rainfall plans with rainfall intensity of 15 mm/h, 30 mm/h and 60 mm/h were made combined with the conditions of artificial rainfall simulation equipment. The designed rainfall test schemes were as follow:

(1) The rainfall durations were same—all were 180 min, but the rainfalls were 45 mm, 90 mm, and 180 mm, respectively, as plotted in Fig. 4 (a).

(2) The rainfalls were same—all were 90 mm, but the rainfall durations were 90 min, 180 min, and 360 min, respectively, as illustrated in Fig. 4 (b).

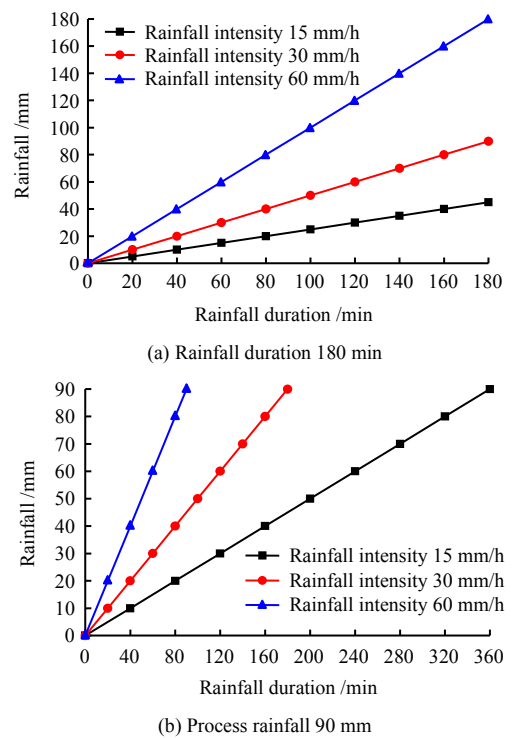


Fig.4 Scheme curves of rainfall and rainfall duration during the test

2.4 Test process

Considering the typical climate of the region and the rainfall characteristics of three rainy seasons, a total of 6 groups and 24 times of experiments on the four soil columns were conducted. The design of test schemes for each group is listed in Table 2.

During the test, the soil column was placed uniformly under the rainfall device to obtain appropriate rainfall uniformity. The wetting front migration in the soil column was measured per 10 minutes. In addition, the soil moisture sensors collected data

automatically every 10 minutes.

**Table 2 Design of testing scheme for each group**

Test number	Test category	Rainfall intensity /( $\text{mm} \cdot \text{h}^{-1}$ )	Rainfall duration /h	Process rainfall /mm	Monitoring duration/h
1	Consistent rainfall duration	15	3.0	45	
2	Consistent rainfall duration	30	3.0	90	
3	Consistent rainfall duration	60	3.0	180	
4	Consistent process rainfall	15	6.0	90	12
5	Consistent process rainfall	30	3.0	90	
6	Consistent process rainfall	60	1.5	90	

### 3 Analysis of test results

#### 3.1 The response law of moisture content to rainfall intensity and duration

##### 3.1.1 The response law of moisture content to rainfall intensity and duration with a given rainfall duration

Figures 5–8 show the time-varying curves of moisture content measured by each moisture sensor when the rainfall duration was 3 hours. After the rain, the moisture sensor continued to monitor for another 9 hours. Tables 3 and 4 list the initial value of moisture content in the soil column test and the sensor response time (from the beginning of rainfall to the moment when the moisture sensor measured the first increase in the moisture content) under the different rainfall intensities.

From Tables 3, 4 and Figs. 5–8, it can be seen that:

(1) The change rate of soil moisture content detected by sensors D1 and D2 is higher than that detected by sensor D3. The sensors D1 and D2 were located in the upper part of the

soil column, and this region had plant roots with good permeability, thus a steep increase of moisture content could be observed. As the rainfall progressed, the moisture content of the upper soil column continued increasing and gradually reached a saturation state. Due to the continuous rainfall, the moisture content still slightly increased after the soil reached saturation. In the later stage of rainfall, the moisture content measured by the sensors D1 and D2 dropped slightly, which was caused by groundwater infiltration.

(2) After the rain, the moisture content of the soil continued increasing, and the increasing rate remained almost unchanged. The upper groundwater infiltrated evenly. When the rain stopped for about 1.5 to 2.0 hours, the peak moisture content was measured by the sensor installed at the upper part of the soil column, and the soil column saturation depth reached 10 cm. After 5 to 6 hours, the peak moisture content was measured by the sensor at the lower part of the soil column, and the wetting front gradually moved down to a depth of 30 cm with rainfall infiltration. In addition, the saturation depth extended downward, and the saturation state finally stabilized in the depth range of the water-proof bottom of the soil column. This reveals the hysteresis characteristics of the eluvial and residual soil landslide under rainfall in the southeastern mountain hills.

(3) The experiment analyzed the infiltration characteristics of soil columns under the condition of 15 mm/h, 30 mm/h, and 60 mm/h rainfall intensities. With the increase of rainfall intensity, the increase rate of soil moisture content grew continuously. After the rain stopped, with the continuous infiltration of groundwater, the moisture content of the lower soil continued increasing, and the moisture content of the upper soil slowly decreased to saturation.

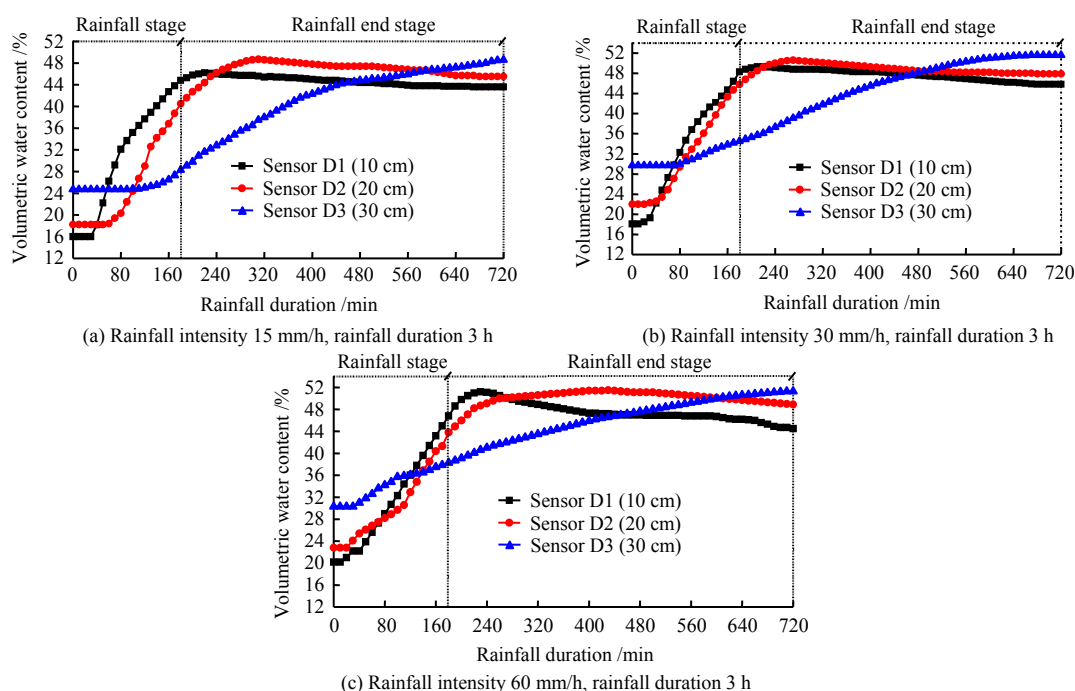


**Fig.5 Time-varying curve of moisture content of soil column MP1 with a specific rainfall duration**

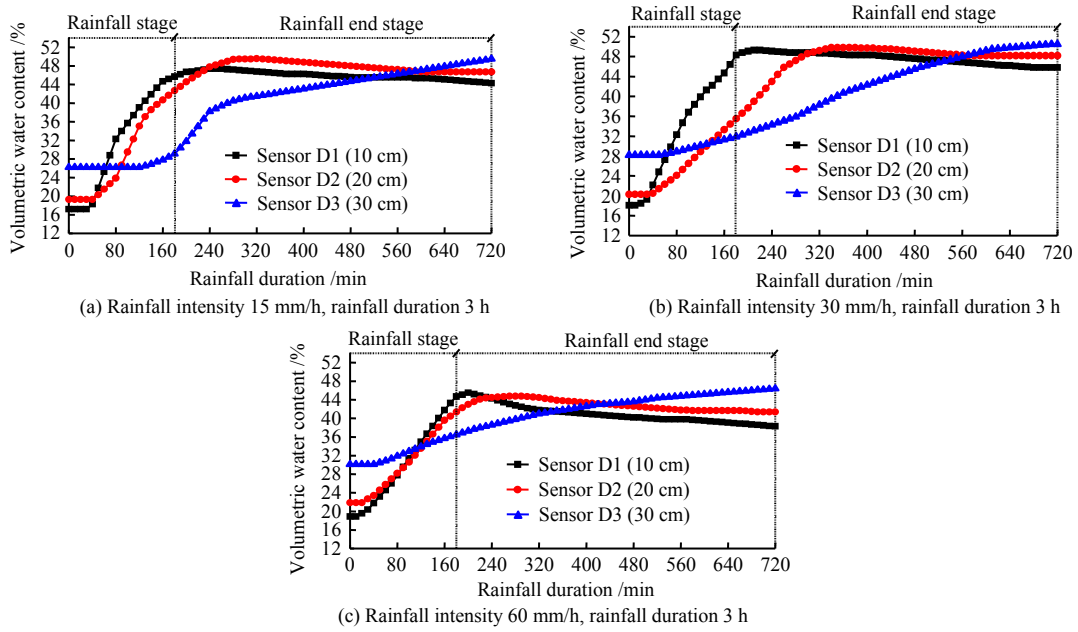


**Fig.6** Time-varying curve of moisture content of soil column NB1 with a certain rainfall duration

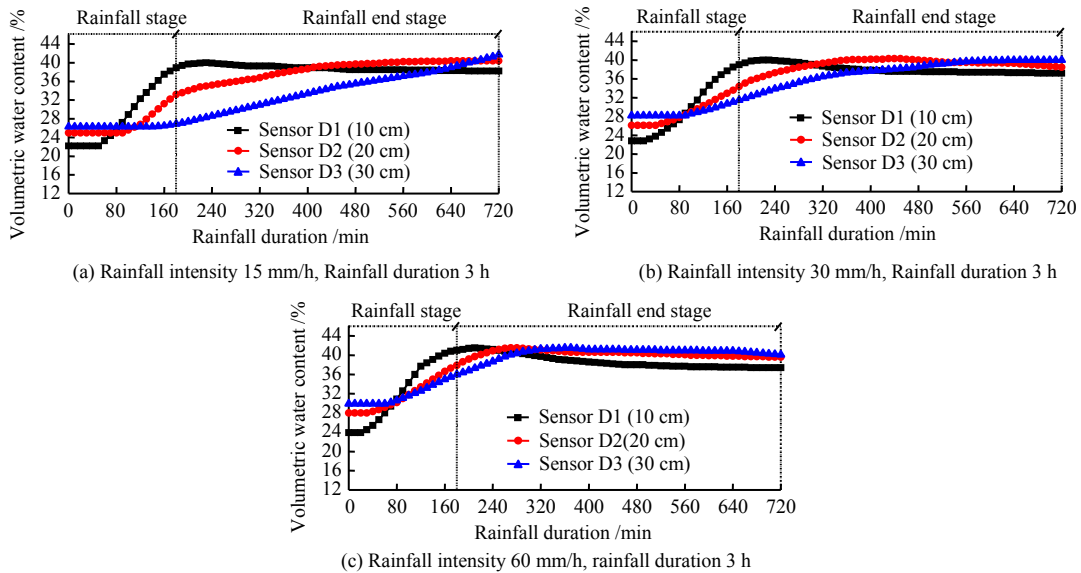


**Fig.7** Time-varying curve of MP2 moisture content of soil column with a specific rainfall duration

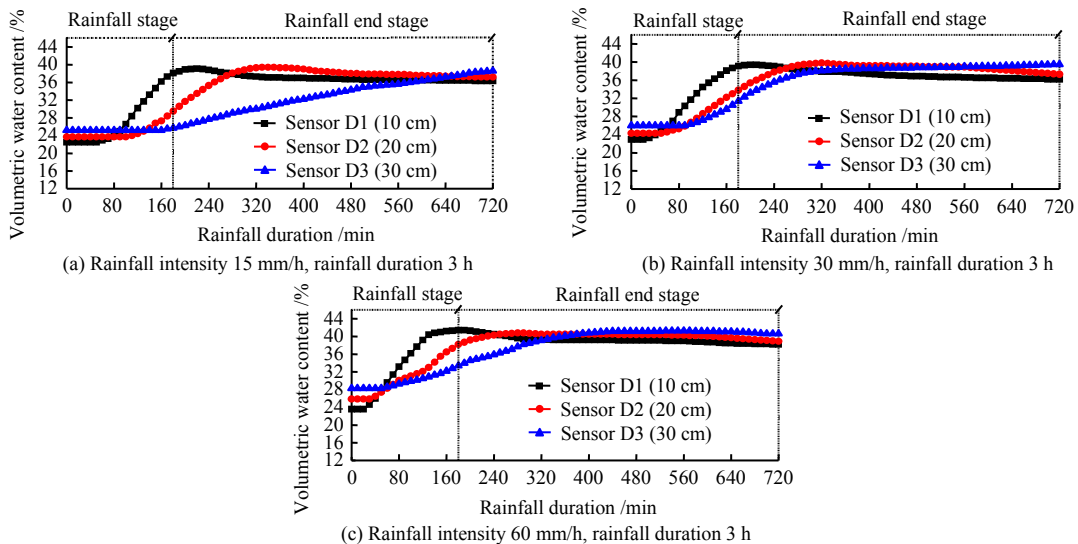


**Fig.8** Time-varying curve of NB2 moisture content of soil column with a specific rainfall duration

**Table 3 Initial values of moisture content and sensor response time of soil columns MP1 and NB1**

Test rainfall intensity /( $\text{mm} \cdot \text{h}^{-1}$ )	Sensor serial number	Soil column MP1		Soil column NB1	
		Initial value of moisture content /%	Sensor response time /min	Initial value of moisture content /%	Sensor response time /min
15	D1	16.0	30	17.2	30
	D2	18.2	50	19.3	40
	D3	24.7	90	26.2	120
30	D1	18.1	20	17.9	20
	D2	22.0	30	20.3	30
	D3	29.7	70	28.2	50
60	D1	20.2	10	18.9	10
	D2	22.8	20	21.9	20
	D3	30.3	30	30.1	40

**Table 4 Initial values of moisture content and sensor response time of soil columns MP2 and NB2**

Test rainfall intensity /( $\text{mm} \cdot \text{h}^{-1}$ )	Sensor serial number	Soil column MP2		Soil column NB2	
		Initial value of moisture content /%	Sensor response time /min	Initial value of moisture content /%	Sensor response time /min
15	D1	22.2	50	22.5	50
	D2	25.0	90	23.7	100
	D3	26.3	140	25.2	170
30	D1	22.8	30	22.9	30
	D2	26.1	40	24.3	50
	D3	28.2	90	26.0	90
60	D1	23.9	20	23.6	20
	D2	28.0	30	25.9	30
	D3	29.9	60	28.3	50

(4) With the increase of the rainfall intensity, the response rate of soil moisture content accelerated, and the growth rate continuously increased. For example, for the soil columns MP1 and NB1, the initial moisture content gradually increased for each group. With increasing the number of the test, the water content remaining in the soil column also accumulated, and the soil inside the soil column was eroded more severely by the water flow, resulting in a constant increase of the permeability coefficient in the test cycle.

### 3.1.2 The response law of moisture content to rainfall intensity and duration with constant process rainfall

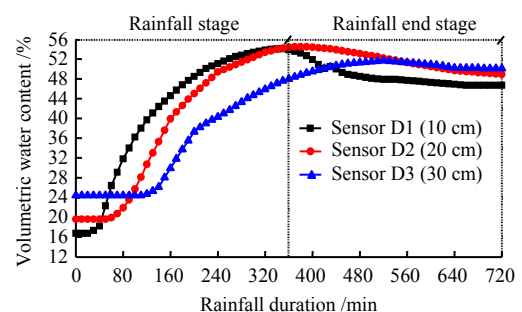
Figures 9–12 present the time-varying curves of the moisture content for each soil column under the constant 90 mm process rainfall. The total rainfall duration of each scheme was 12 hours, which was consistent with the plan of the same rainfall duration to ensure the comparability for different test plans.

(1) When the process rainfall was same, the effective infiltration amount of rainwater under the condition of low rainfall intensity and long duration (15 mm/h) was greater than that under the condition of 30 mm/h and 60 mm/h rainfall intensities. The saturated state of each soil column was very obvious under the 15 mm/h rainfall intensity, and the peak

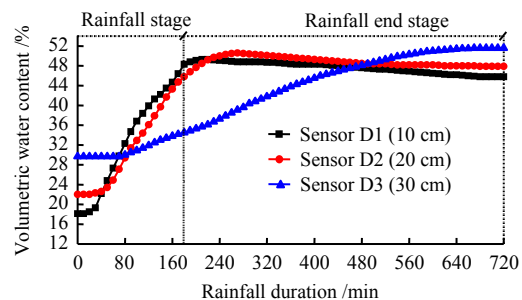
moisture content could reach 54%, while the peak moisture content for 30 mm/h and 60 mm/h were only 50.2% and 38.5%, respectively.

(2) For the low rainfall intensity and long duration case, the soil moisture content changed greatly, and the rainwater effective infiltration amount was larger. The effect of rainfall with heavy rainfall intensity and short duration on the soil was mainly related to the initial moisture content and the pore structure of the soil. The rainfall with low intensity and long duration could infiltrate into soil evenly. Under the condition of heavy rainfall intensity, when the rainfall intensity was greater than the infiltration capacity, the remaining water would flow along the surface, forming a saturated and surplus overland flow<sup>[17]</sup>. Since the rainfall could not infiltrate in time, the heavy rainfall overflowed from the barrel in the experiment, and the effective infiltration rainfall decreased.

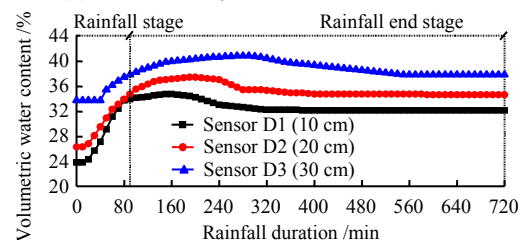
(3) When the rainfall intensity was constant, the rainfall infiltration amount increased with the rainfall duration. For example, under the condition of 15 mm/h rainfall intensity, the soil reached saturation when the rainfall duration was 3 hours. As the rainwater continued to infiltrate, the peak moisture content was 48%. When the rainfall duration reached 6 hours, the peak moisture content could reach 53.1%.



(a) Rainfall intensity 15 mm/h, rainfall duration 6 h



(b) Rainfall intensity 30 mm/h, rainfall duration 3 h



(c) Rainfall intensity 60 mm/h, rainfall duration 1.5 h

**Fig.9 Time-varying curves of moisture content of soil column MP1 with constant process rainfall**

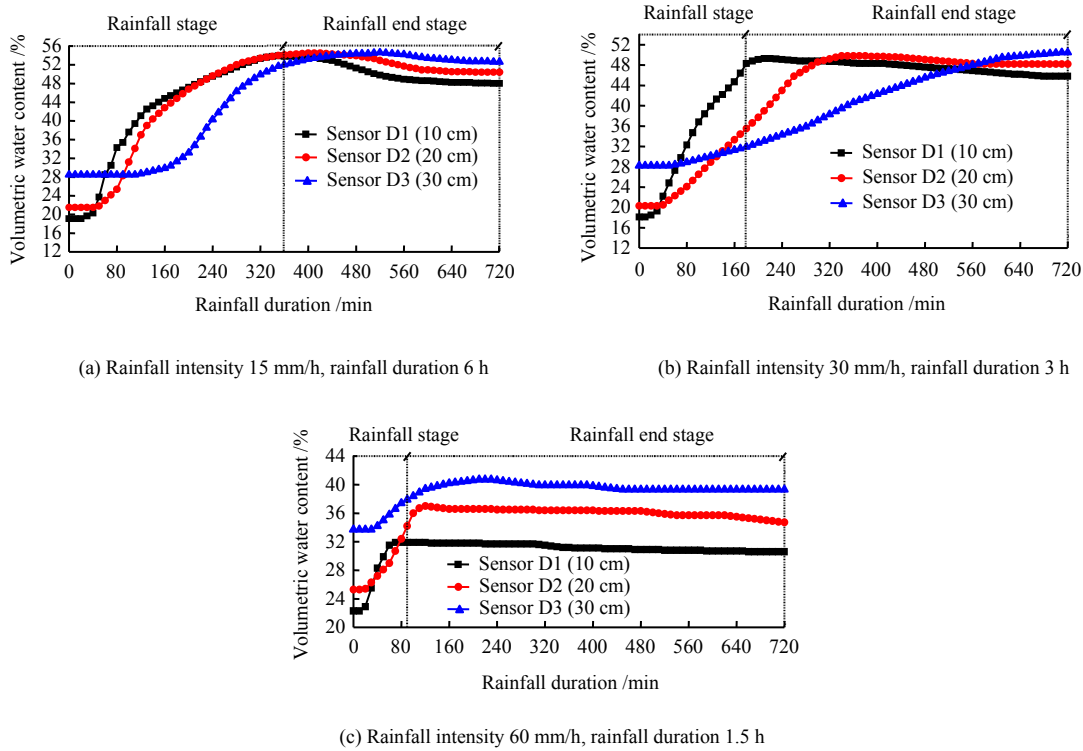


**Fig.10** Time-varying curves of moisture content of soil column NB1 with constant process rainfall

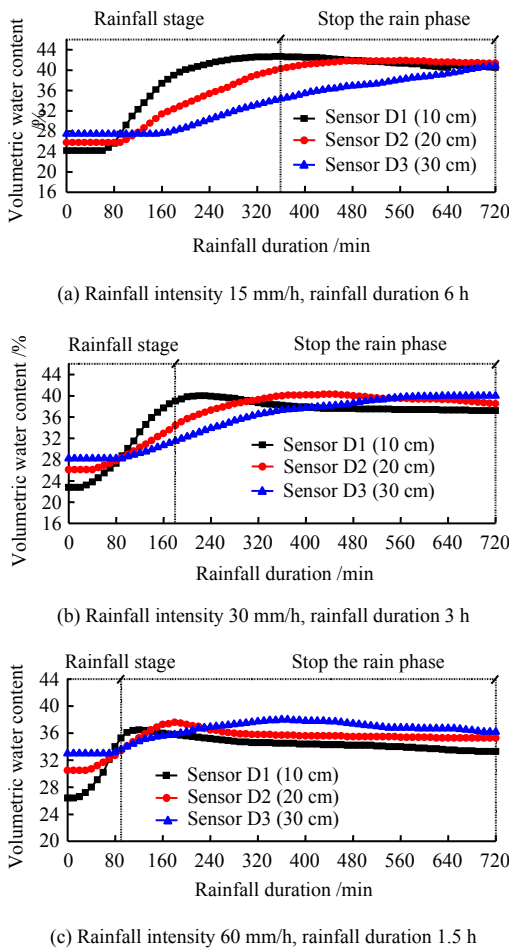


**Fig.11** Time-varying curves of moisture content of soil column MP2 with constant process rainfall

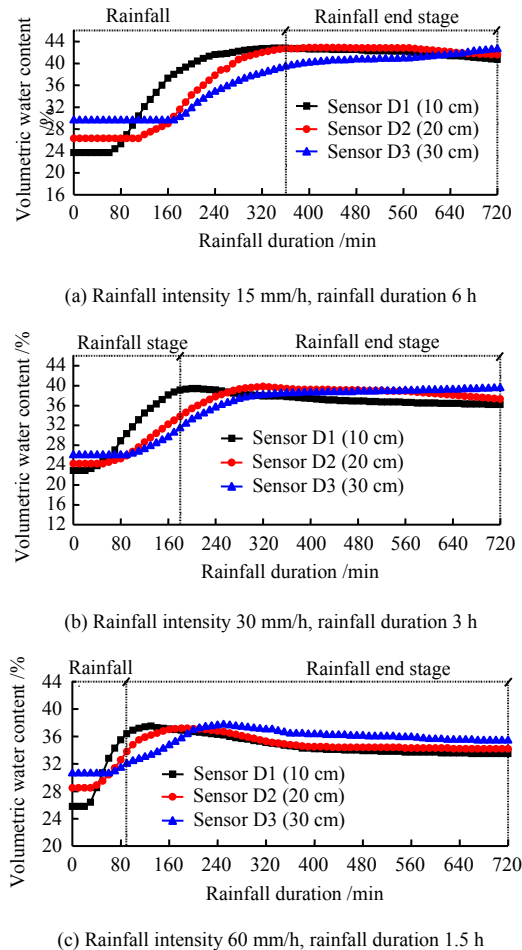


**Fig.12** Time-varying curves of moisture content of soil column NB2 with constant process rainfall

### 3.2 The response law of wetting front to rainfall intensity and duration

The wetting front is an important index to study the infiltration characteristics of the soil under rainfall. Generally, the interface between the wet area in the soil and the natural soil is defined as wetting front.

#### 3.2.1 The response law of wetting front to rainfall intensity with a given rainfall duration

Figure 13 shows the time-varying law curve of wetting front migration of the soil column under the same rainfall duration condition. It has the following characteristics:

(1) As the rain progressed, the wetting front of each soil column moved down and expanded along the soil column. In the early stage of rainfall, the migration rate of the wetting front was relatively fast. But after the infiltration depth reached 20–30 cm, the infiltration rate of the soil wetting front decreased significantly and tended to be gentle gradually.

(2) With the increase of rainfall intensity, the infiltration depth of wetting front of soil column became larger. In the condition of rainfall duration 180 min, for the rainfall intensity of 15 mm/h, the wetting front migrated faster in the shallow soil body in the early stage, and then slowed down, correspondingly, the wetting front of soil column MP1 was 34 cm, and that of soil column NB1 was 32 cm; for the rainfall intensity of

30 mm/h, the wetting front of soil column MP1 was 38 cm, and that of soil column NB1 was 39 cm; and for the rainfall intensity of 60 mm/h, the wetting front of soil column MP1 was 40 cm, and that of soil column NB1 was 42 cm.

(3) Under the condition of different rainfall intensities, the wetting front migration velocity of residual soil column was relatively uniform. With the continuation of rainfall (increasing the rainfall duration), the wetting front depth became deeper and deeper. When the rainfall intensity was 15 mm/h, which is close to the permeability coefficient of the residual soil, the wetting front migration was relatively uniform, and the response time-varying curve was relatively smooth, as shown in Fig.13. When the rainfall intensity was 30 mm/h, in the shallow soil, the migration rate of the wetting front curve was fast because of the relatively low moisture content and strong water absorption. After entering the deep soil, the migration speed of the wetting front slowed down to some extent, but it was still relatively stable. When the rainfall intensity was 60 mm/h, which was slightly greater than the permeability coefficient of the residual soil, the wetting front infiltrated faster in the shallow layer, and the migration speed slowed down slightly in the deeper layers. At this time, the accumulated water on the top of the soil column drained out.

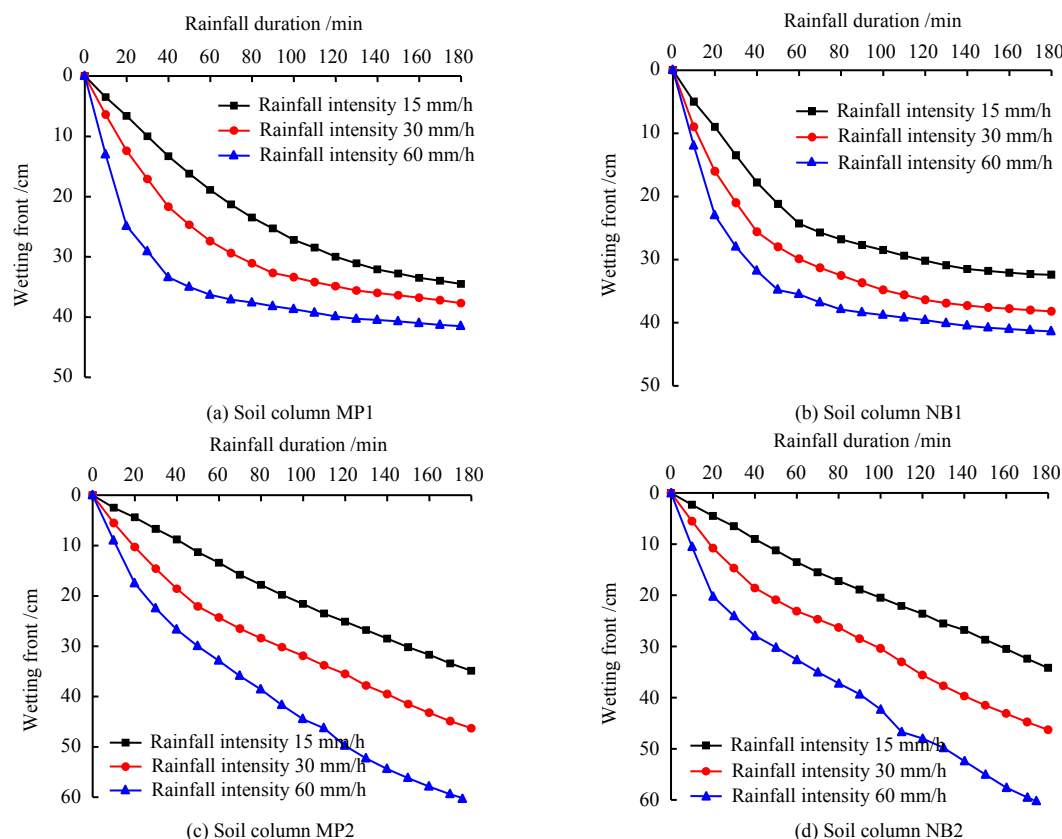


Fig.13 Time-dependent curves of wetting front for different soil columns within rainfall duration of 3h

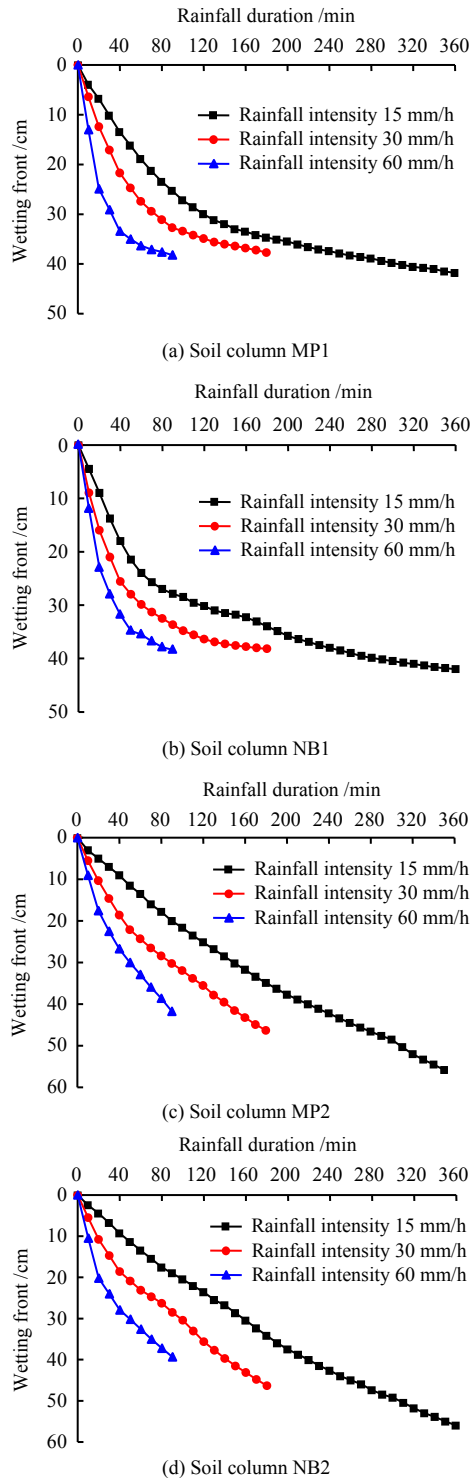
#### 3.2.2 The response law of wetting front to rainfall intensity with constant process rainfall

Figure 14 shows the time-varying law curves of wetting front

migration for different soil columns under the same process rainfall condition. It has the following characteristics:

(1) Because of the large permeability coefficient of the

shallow soil, the rainfall could infiltrate rapidly in the shallow layer under the different rainfall intensities. After the wetting front reached 30 cm, the rainfall infiltrated into the deeper soil layers and stayed in this interval with a slow infiltration.



**Fig.14 Time-dependent curves of wetting front for different soil columns within rainfall duration of 6h**

(2) The longer the rainfall duration, the deeper the rainfall infiltration depth. The wetting front depths of soil column MP1 were 36 cm, 37 cm, 41 cm, and the wetting front depths of soil column NB1 were 39 cm, 39 cm, 42 cm, respectively, for the

rainfall duration of 1.5, 3, and 6 hours.

(3) By comparing the wetting front curves of soil columns in Figs.13 and 14, it is found that rainfall duration had little effect on the wetting front depth when the permeability coefficient of soil layers was relatively small, and the rainfall infiltration was mainly controlled by the permeability coefficient of the soil itself. For example, under the condition of the rainfall intensity of 15 mm/h, the wetting front of soil column MP1 with a low permeability coefficient moved downwards 7 cm more in rainfall duration of 6 hours than that in 3 hours; similarly, the soil column NB1 moved down 10 cm more.

(4) It can be seen from Fig.14 that when the rainfall intensity was close to the soil permeability coefficient, the longer the rainfall duration, the larger the range of rainfall infiltration, and also the deeper the wetting front migration depth. For example, the wetting front depths of soil columns MP1 and NB1 increased by 7 cm and 8 cm, respectively, when the rainfall intensity was 15 mm/h and the rainfall duration was 6 hours, compared with the condition of rainfall duration of 3 hours. As shown in Figs.14(a) and 14(b), because the permeability coefficient in the soil was close to the rainfall intensity, the rainfall could infiltrate easier, and the migration curve of the wetting front of soil columns was relatively straight, and also the migration rate of the wetting front was relatively large.

### 3.2.3 The transition process from unsaturated state to saturated state of soil column

From the experimental response laws of the soil column moisture content and the wetting front to rainfall intensity and duration, the transformation mechanism of the soil column from unsaturated state to saturated state can be further analyzed. The soil column was in unsaturated state before rainfall infiltration, and the rainfall infiltration was mainly controlled by matrix potential and gravity potential<sup>[18]</sup>. The rainfall infiltration of the soil column experienced three stages. (1) At the early stage of infiltration, the matrix potential played a leading role, and the infiltrated water was absorbed by the soil particles, and further translated into film water, forming the wetting front. (2) The infiltration of water caused an unstable flow within the pores of the soil, and the wetting front advanced downward at a higher rate, and further gradually filled the pores. (3) At the later stage, the gravity potential played a more important role. The water flowed steadily under the action of gravity. After entering the stable seepage stage, with the increase of time, the nearly saturated water in the upper layer of the soil gradually moved down, and the wetting front descended, and then the lower part of the soil column reached the saturated state.

### 3.2.4 The infiltration formula of soil wetting front

According to the time-varying data of the wetting front

observed in the experiment, the first-order, second-order or third-order fitting on the relationship between the wetting front depth and time were carried out. The characteristic index of fitting degree was  $R^2$ , and the fitting convergence condition was  $R^2 > 0.95$ <sup>[19]</sup>. The infiltration formulas of wetting front depth for each soil column are listed in Tables 5–8.

By analyzing the results mentioned above, it can be found that when the rainfall intensity is low, the wetting front depth has a strong linear relationship with time. With the increase of rainfall intensity, the linear relationship between the wetting front depth and time gradually weakens. In addition, the linear relationship of the residual soil is stronger than that of the colluvial soil. As for the colluvial soil, the permeability coefficient of the surface layer is large, while the permeability coefficient of the deep layer is small. Under the condition of low rainfall intensity, the wetting front shows a second-order function relationship with time, while under the condition of heavy rainfall intensity, the wetting front shows a third-order function relationship with time, and the infiltration rate decreases significantly. As for residual soil, the permeability coefficient is uniform across the soil. Under the condition of low rainfall intensity, the wetting front has a strong linear relationship with time, while under the condition of heavy rainfall intensity, the wetting front shows a second-order function relationship with time, and the infiltration rate also decreases slightly.

**Table 5 Soil column MP1 infiltration formula**

Infiltration formula of wetting front of slopewash soil in Maping landslide	Fitting degree $R^2$	Applicability	
		Rainfall intensity $/(mm \cdot h^{-1})$	Soil permeability level
$h = -0.001 0t^2 + 0.373 8t - 0.075 6$	0.99	15	Hard permeable
$h = -0.001 7t^2 + 0.487 0t + 2.502 5$	0.98	30	
$h = 0.000 03t^3 - 0.009 6t^2 + 1.061 3t + 2.902 7$	0.96	60	

In the formula:  $h$  is the infiltration depth of wetting front (mm);  $t$  is the rainfall duration (min).

**Table 6 Soil column NB1 infiltration formula**

Infiltration formula of wetting front of slopewash soil in Neiban landslide	Fitting degree $R^2$	applicability	
		Rainfall intensity $/(mm \cdot h^{-1})$	Soil permeability level
$h = -0.001 5t^2 + 0.432 0t + 1.331 9$	0.98	15	Hard permeabler
$h = -0.001 8t^2 + 0.506 2t + 4.307 7$	0.95	30	
$h = 0.000 03t^3 - 0.009 1t^2 + 1.029 9t + 2.535 2$	0.96	60	

**Table 7 Soil column MP2 infiltration formula**

Infiltration formula of wetting front of residual soil in Maping landslide	Fitting degree $R^2$	Applicability	
		Rainfall intensity $/(mm \cdot h^{-1})$	Soil permeability level
$h = 0.194 8t + 1.069 1$	0.99	15	Weak permeable
$h = 0.238 8t + 6.324 5$	0.97	30	
$h = -0.001 4t^2 + 0.559 5t + 3.748 3$	0.98	60	

**Table 8 Soil column NB2 infiltration formula**

Infiltration formula of wetting front of residual soil in Neiban landslide	Fitting degree $R^2$	applicability	
		Rainfall intensity $/(mm \cdot h^{-1})$	Soil permeability level
$h = 0.186 3t - 1.173 4$	0.99	15	Weak permeable
$h = 0.239 1t + 5.860 5$	0.98	30	
$h = -0.002 6t^2 + 0.607 3t + 4.815 1$	0.97	60	

## 4 Conclusion

In this research, the permeability characteristics of the representative slope wash soil and granite residual soil from two typical geological disaster points were investigated experimentally by the self-developed soil column infiltration test devices. Two test plans including same rainfall duration but different rainfall intensities (15 mm/h, 30 mm/h and 60 mm/h), and same rainfall (90 mm) but different rainfall intensities were designed to analyze the response laws of the moisture content, wetting front and infiltration rate, etc.

(1) During the rainfall infiltration, the soil moisture content responded to the rainfall step by step, from shallow to deep layer. The soil moisture content increased continuously in the process of rainfall, and the moisture content of the deep soil continued increasing to saturation after rainfall. After a period of time, the water continued to infiltrate and evaporate, which made the soil moisture content gradually decrease. The influence of rainfall intensity on moisture content mainly presented in the first response time and the saturation speed. Specifically, the greater the rainfall intensity was, the shorter the response time would be, and the faster the saturation speed would be. When the process rainfall was insufficient, the soil could not be saturated. With the constant increasing of the experiment cycle and the rainfall frequency, the soil would saturate faster due to the early rainfall accumulation effect.

(2) The wetting front of the soil was closely related to the permeability of the soil itself and rainfall intensity. A larger soil permeability coefficient and a greater rainfall intensity caused a deeper wetting front and a faster spreading rate. When the rainfall reached a certain intensity or lasted for a certain duration, the soil moisture content increased greatly, and then the migration velocity of the soil wetting front had a downward trend.

(3) The wetting front infiltration formulas of soil column showed that when the rainfall intensity was small, the wetting front depth had a strong linear relationship with the rainfall duration. With the increase of the rainfall intensity, the linear relationship between the wetting front depth and time gradually weakened, showing a second-order function relationship.

(4) The rainfall infiltration test of the undisturbed soil column will be of great theoretical and practical significance in the following three aspects: (i) further revealing the rainfall infiltration response law of the slope wash and residual soil

under the action of typhoon and rainstorm in the study area; (ii) disclosing the transition mechanism from unsaturated state to saturated state of the slope wash and residual soil; (iii) helpful for the precise monitoring and early warning of rainfall-type landslide.

## References

- [1] LUMB P. Effect of rain storms on slope stability[M]. Hong Kong: Local Property & Printing Company Limited, 1962.
- [2] LI Ai-guo, YUE Zhong-qi, TAN Guo-huan, et al. Soil moisture and suction measurement and its effect on slope stability[J]. *Chinese Journal of Geotechnical Engineering*, 2003, 25(3): 278–282.
- [3] YAN Shao-jun, TANG Hui-ming, XIANG Wei. Effect of rainfall on the stability of landslides[J]. *Hydrogeology & Engineering Geology*, 2007, 34(2): 33–36.
- [4] YEH HSINFU, LEE CHENCHANG, LEE CHENGHAW. A rainfall-infiltration model for unsaturated soil slope stability[J]. *Journal of Environmental Engineering and Management*, 2008, 18(4): 261–268.
- [5] LI Ning, XU Jian-cong, QIN Ya-zhou, Research on calculation model for stability evaluation of rainfall-induced shallow landslides[J]. *Rock and Soil Mechanics*, 2012, 33(5): 1485–1490.
- [6] HAN Tong-chun, MA Shi-guo, XU Ri-qing. Research on delayed effect of landslides caused by air pressure under heavy rainfall[J]. *Rock and Soil Mechanics*, 2013, 34(5): 1360–1366.
- [7] WEN Ming-sheng, WANG Lian-jun, LI Tie-feng, et al. Real-time monitoring based landslide monitoring system at Hekou sugar refinery factory[J]. *Journal of Engineering Geology*, 2011, 19(1): 76–82.
- [8] ZHOU Zhong, WANG Hong-gui, FU He-lin, et al. Influences of rainfall infiltration on stability of accumulation slope by in-situ monitoring test[J]. *Journal of Central South University of Technology*, 2009, 16(2): 297–302.
- [9] LI Ru-cheng, WANG Fu-ming. Effect of rainfall infiltration on stability of mudstone-soil mixture embankment[J]. *Chinese Journal of Rock Mechanics and Engineering*, 2008, 27(11): 2260–2266.
- [10] ZHENG Jian-hao, ZHANG Zhi-bin, YUAN Jun-ping. Dynamic monitoring of soil suction in high slope of residual soil during rainfall[J]. *Journal of China & Foreign Highway*, 2006, 26(2): 47–50.
- [11] ZHAN Liang-tong, WU Hong-wei, BAO Cheng-gang, et al. Artificial rainfall infiltration tests on a well-instrumented unsaturated expansive soil slope[J]. *Rock and Soil Mechanics*, 2003, 24(2): 151–158.
- [12] REN Ke-bin, WANG Bo, LI Xin-ming, et al. Strength properties and pore-size distribution of earthen archaeological site under dry-wet cycles of capillary water[J]. *Rock and Soil Mechanics*, 2019, 40(3): 962–970.
- [13] HU Ting-fei, WANG Hui, HU Chuan-wang, et al. Effect of thickness of gravel cover on infiltration characteristics of water repellent soils and its model optimization[J]. *Journal of Soil and Water Conservation*, 2019, 33(2): 17–29.
- [14] CHENG Qin-bo, CHEN Xi, ZHANG Zhi-cai, et al. Analytic solution for 1D convection-dispersion equation with time-variable boundary and its application in soil column experiment[J]. *Journal of Hohai University (Natural Sciences)*, 2018, 46(6): 486–491.
- [15] WEI Zhen, LI Gong-sheng, CHI Guang-sheng. A mathematical model for a disturbed soil-column experiment and numerical simulations for parameters inversion[J]. *Journal of Shandong University of Technology (Natural Science Edition)*, 2009, 23(2): 1–6.
- [16] Ministry of Water Resources of the People's Republic of China. GB/T50123 — 1999 Standard for soil test method[S]. Beijing: China Planning Press, 1999.
- [17] NING LU, JONATHAN W GODT. Hillslope hydrology and stability[M]. Translated by JIAN Wen-xing, WANG Jing-e, HOU Long. Beijing: Higher Education Press, 2013.
- [18] SHAO Ming-shen, PEI Qiang-qiang, WANG Si-jing, et al. Field tests of PS infiltration for unsaturated earthen sites[J]. *Dunhuang Research*, 2012(3): 116–121.
- [19] LUO Yang-hua. Analysis of seepage and stability on unsaturated residual soil slope under slope under rainfall[D]. Fuzhou: Fuzhou University, 2016.